Asian Journal of Andrology (2024) 26, 25–33
www.asiaandro.com; https://journals.lww.com/ajandrology

Open Access

ORIGINAL ARTICLE

Sperm Biology

Decreased AKAP4/PKA signaling pathway in high DFI sperm affects sperm capacitation

Kun Zhang[1,2,*], Xiu-Hua Xu[1,*], Jian Wu[1], Ning Wang[1], Gang Li[3], Gui-Min Hao[1], Jin-Feng Cao[1]

The sperm DNA fragmentation index (DFI) is a metric used to assess DNA fragmentation within sperm. During *in vitro* fertilization-embryo transfer (IVF-ET), high sperm DFI can lead to a low fertilization rate, poor embryo development, early miscarriage, *etc*. A kinase anchoring protein (AKAP) is a scaffold protein that can bind protein kinase A (PKA) to subcellular sites of specific substrates and protects the biophosphorylation reaction. Sperm protein antigen 17 (SPA17) can also bind to AKAP. This study intends to explore the reason for the decreased fertilization rate observed in high sperm DFI (H-DFI) patients during IVF-ET. In addition, the study investigates the expression of AKAP, protein kinase A regulatory subunit (PKARII), and SPA17 between H-DFI and low sperm DFI (L-DFI) patients. SPA17 at the transcriptional level is abnormal, the translational level increases in H-DFI patients, and the expression of AKAP4/PKARII protein decreases. H_2O_2 has been used to simulate oxidative stress damage to spermatozoa during the formation of sperm DFI. It indicates that H_2O_2 increases the expression of sperm SPA17 protein and suppresses AKAP4/PKARII protein expression. These processes inhibit sperm capacitation and reduce acrosomal reactions. Embryo culture data and IVF outcomes have been documented. The H-DFI group has a lower fertilization rate. Therefore, the results indicate that the possible causes for the decreased fertilization rate in the H-DFI patients have included loss of sperm AKAP4/PKARII proteins, blocked sperm capacitation, and reduced occurrence of acrosome reaction.

Asian Journal of Andrology (2024) **26**, 25–33; doi: 10.4103/aja202329; published online: 15 August 2023

Keywords: AKAP; PKA; SPA17; sperm capacitation; sperm DNA fragmentation index

INTRODUCTION

The sperm DNA fragmentation index (DFI) is a metric used to assess DNA fragmentation in sperm. Recent clinical data show that a high sperm DNA fragmentation index (H-DFI) is strongly associated with fertilization rate,[1] pregnancy rate,[2] and miscarriage rate[3,4] during *in vitro* fertilization-embryo transfer (IVF-ET). H-DFI semen samples often show abnormal sperm motility[5] and morphology.[6] These characteristics can lead to a low fertilization rate, poor embryo development, early miscarriage, and other issues during IVF-ET. Among the many causes of sperm DFI, oxidative stress (OS) is considered the most important damaging factor.[7] Reactive oxygen species (ROS) are reactive oxygen metabolites produced by sperm during normal physiological processes. OS is an imbalance in the ratio of ROS to antioxidant substances in the sperm microenvironment. Excessive ROS can cause serious DNA damage to sperm. A large number of DNA breaks are produced and the sperm itself cannot repair this damage. Moreover, ROS can also result in redox modifications of lipids, which alters the sperm's plasma membrane and intracytoplasmic proteins,[8] which impacts important sperm physiological functions, such as acrosomal exocytosis, sperm capacitation, and fertilization. However, it is still unclear how OS affects these processes, what kind of damage is mainly caused, and what potential effects this damage has during IVF-ET. This study investigates the mechanisms that probably drive H-DFI-induced complications during the IVF-ET process and the functional impairment of sperm associated with OS.

Sperm capacitation is a complex series of reactions that ejaculated spermatozoa undergo in the female reproductive tract during fertilization, accompanied by the production of the sperm's own ROS, a vital process for sperm maturation and a prerequisite for fertilization.[9] ROS is significant in sperm capacitation, but the current understanding of the biochemical pathways linking bicarbonate, ROS, cyclic adenosine monophosphate (cAMP) generation, protein kinase A (PKA) activation, protein phosphorylation, and capacitation still contains many gaps.[10] The term ROS covers a variety of oxygen metabolites, such as the superoxide anion and hydrogen peroxide. Superoxide dismutase (SOD) catalyzes the dismutation of superoxide anion into hydrogen peroxide.[11] The action of ROS on mammalian sperm capacitation is bicarbonate dependent. The combination of O_2^-, HCO_3^-, and Ca^{2+} activates soluble adenylyl cyclase, thereby stimulating cAMP production and the activation of PKA.[12] After PKA is activated, it can act on tyrosine kinase, causing tyrosine groups attached to sperm proteins to develop biophosphorylation reactions. The accumulation of a series of processes, such as massive tyrosine phosphorylation and calcium influx, eventually induces sperm to experience hyperactivated motility (HAM), which is one of the endpoints of sperm capacitation.[13] Only capacitated spermatozoa can undergo the acrosome reaction in the vicinity of the egg.[14]

[1]Hebei Key Laboratory of Infertility and Genetics, Department of Reproductive Medicine, Second Hospital of Hebei Medical University, Shijiazhuang 050000, China; [2]Department of Reproductive Medicine, Affiliated Hospital of Xuzhou Medical University, Xuzhou 221000, China; [3]Department of Neurology, The 980th Hospital of the People's Liberation Army Joint Logistics Support Force (Bethune International Peace Hospital), Shijiazhuang 050000, China.
*These authors contributed equally to this work.
Correspondence: Dr. JF Cao (jfcaoc@126.com)
Received: 12 March 2023; Accepted: 12 June 2023

PKA is a serine/threonine kinase commonly expressed in humans and is an important, highly conserved protein in eukaryotes. PKA is a tetrameric holoenzyme composed of four different subunits, including two regulatory subunits, RI and RII, and two catalytic subunits, C1 and C2. In spermatozoa, activation of PKA occurs following interaction with cAMP, and there is a phosphorylation site on the R subunit. Therefore, when cAMP binds to the R subunit, protein conformation is changed, and active catalytic subunits are released to phosphorylate downstream targets.[15,16]

During sperm capacitation, the activation of PKA is strictly spatiotemporally regulated to ensure the correct functioning of the signaling pathway.[17] A dimerization docking domain (D/D) exists at the N-terminus of the RII subunit, which can noncovalently bind to the AKB structural domain on the A-kinase anchoring protein (AKAP), linking PKA to AKAP.[18] AKAP can precisely direct PKA to subcellular sites of specific substrates and adjust its localization sequence, isolating the reaction from other substrates. It can also degrade cAMP to block the effect of PKA after the reaction, in addition to protecting PKA from premature activation by other substances and from proteasomal degradation.[19,20] As a scaffolding protein, AKAP not only has a PKA-binding domain, but also has other binding sites that can interact with protein kinases, protein phosphatases,[21] and ion channels to form a supramolecular complex. Therefore, AKAP can serve as a platform for the integration of the cAMP-PKA pathway[22] and other signaling pathways. AKAP3 and AKAP4 are mainly expressed in mature spermatozoa and are distributed within the flagellum and acrosomal regions of the spermatozoa.[23] In *AKAP4*-knockout mice, males are found to be sterile. Although spermatogenesis is normal, sperm has no forward motion and a shortened tail curl, suggesting that AKAP4 is irreplaceable for male reproductive function.[24]

Sperm protein antigen 17 (SPA17) is a sperm protein mainly expressed within germ cells and it has a dimerization docking binding domain, similar to that of protein kinase A regulatory subunit (PKARII), at its N-terminus that can bind SPA17 to AKAP3 and AKAP4.[25] SPA17 is mainly seen both in the head cytoplasm and throughout the tail region of sperm.[26] In addition to sperm, SPA17 is expressed in many different cell types, such as ciliated cells and tumor cells.[27] It is strongly associated with cell motility, migration, and adhesion functions.[28] Since it is found in a variety of tumor cells, some experts believe that SPA17 may be considered a "carcinoembryonic antigen."[29] Although some aspects of SPA17 have been identified, its expression mechanism remains unclear. In an earlier study, the primary function of SPA17 was related to oocyte zona pellucida binding.[30] However, subsequent analysis suggests that SPA17 plays a regulatory role through binding to AKAP proteins to form a complex, and therefore the role of SPA17 in zona pellucida binding is not a major one.[31]

Previous reports have indicated that AKAP, PKA, and SPA17 play important roles in sperm capacitation. Nixon *et al.*[32] and Baker *et al.*[33] reported that AKAP4 and PKA are susceptible to oxidative modification by ROS, and Lee *et al.*[25] reported that *Akap4*-knockout mice had increased SPA17 expression. However, these studies[32–34] did not investigate the expression of SPA17 under the influence of high ROS levels on AKAP. This study has focused on how high levels of ROS in H-DFI patients affect AKAP4, PKA, and SPA17 expression, and whether this ultimately affects IVF-ET outcomes and sperm function.

PARTICIPANTS AND METHODS

Ethical approval

Studies involving human participants were reviewed and approved by the Ethics Committee of the Second Hospital of Hebei Medical University (Shijiazhuang, China; Approval No. 2019-R160). All methods performed were in accordance with relevant guidelines and regulations of the Declaration of Helsinki (2008 version). The informed consent form was obtained from each participant as per the directions of the Chinese Ministry of Public Health.

Reagents

SpermGrad, Spermrinse, G-MOPS, G-1, G-2, and G-IVF PLUS were purchased from Vitrolife (Goteborg, Sweden); MonAmp™ RNA Extraction Reagent, MonAmp™ Reverse Transcription Kit, and MonAmp™ ChemoHS qPCR Mix were purchased from Monad (Wuhan, China). SPA17 rabbit polyclonal antibody, phosphorylated protein kinase B (p-AKT) rabbit polyclonal antibody, and AKT rabbit polyclonal antibody were purchased from Proteintech (Rosemont, CA, USA). Horseradish peroxidase (HRP)-labeled sheep anti-rabbit antibody and sheep anti-mouse antibody were also purchased from Proteintech and PKARII antibody was purchased from Abcam (Cambridge, UK).

The target gene DNA sequences were retrieved using the National Center for Biotechnology Information (NCBI) database and then primers were designed by Primer5.0. Next, primers were synthesized by Sangon Biotech (Shanghai, China; **Supplementary Table 2**).

Study population

Semen collection was from 179 male patients treated with IVF-ET for female tubal factors between September 2020 and January 2021 at the Department of Reproductive Medicine at the Second Hospital of Hebei Medical University. The inclusion criteria adopted were: female partner's age ≤38 years; partners had normal karyotype test; the number of assisted reproductive technology cycles ≤2; and the number of oocytes retrieved in the current cycle ≥4. Exclusion criteria included factors that affect pregnancy, such as the female combination of polycystic ovary syndrome, endometriosis, hyperprolactinemia, uterine fibroids, uterine structural abnormalities, hydrocele, and uterine adhesions; and factors affecting embryonic development, such as leukocytospermia. The male patients were grouped according to their sperm DFI test value on the day of oocyte retrieval, and ≤15% were divided into the L-DFI group (n = 137), and ≥30% into the H-DFI group (n = 42).

Semen density gradient centrifugation (DGC) processing

The 90% gradient solution (1.5 ml) was in the lower lever, 1.5 ml of the 45% gradient solution was in the upper lever, and an appropriate amount of fully liquefied semen was in the upper layer of the gradient solution. The gradient solution-sperm mixture was then centrifuged (Zhongke, Hefei, China) at 500*g* for 10 min to remove the upper two layers of liquid. The precipitate was resuspended with 5 ml of sperm rinse solution and then centrifuged at 300*g* for 10 min. The sperm rinse solution was removed, leaving sperm deposits.

IVF

After oocyte retrieval, cumulus-oocyte complexes were collected and rinsed with G-MOPS (Vitrolife). Oocytes were incubated at 37°C, 5% CO_2, and 95% air humidity for 1–3 h. The insemination tray was added an appropriate amount of sperm suspension. After 5–6 h, the oocytes are removed and placed in another microdrop. The second polar body of oocytes can be observed. After 17 ± 1 h of insemination, oocytes containing two pronuclei (2PN) were normally fertilization. Embryos on day 3 (D3) were scored according to the morphological characteristics and the scoring method of the Bourn Hall Clinic in the UK. Next, high-quality embryos (n=1 or 2) were selected for transfer. The remaining embryos were cryopreserved using a vitrification kit (KITAZATO BioPharma, Shizuoka, Japan) or continued in blastocyst culture. Blastocysts were scored on day 5 (D5) or day 6 (D6) using the

scoring system of Gardner and Schoolcraft (2000).[35] Blastocysts of good quality were cryopreserved, and those of poor quality were discarded.

Semen analysis and morphology assessment

Fresh semen was liquefied at 37°C for 30–60 min. The liquefied semen was mixed completely. Semen slides were prepared with about 5–10 μl for sperm morphology evaluation. Sperm Morphology Kit (Huakang, Shenzhen, China) was used for Diff-Quik rapid staining. The percentage of normal sperm and abnormal sperm in the head, neck, midsection, and tail were counted. A total of 10 μl semen was added to a 20 μm deep Markler sperm counting plate. The semen was analyzed by a computer-assisted sperm analyzer (CASA) testing system (Dynamic Analysis System version 7.3, Weili, Beijing, China). Sperm concentration, the total number of forward motile sperm, the total number of immobile sperm, and the total sperm motility rate were calculated. Semen was analyzed and assessed according to the 5th edition of the World Health Organization (WHO) laboratory manual.[36]

Sperm DFI test

Sperms were processed using a sperm DNA fragmentation test kit. The Sperm DNA Fragmentation Staining Kit was purchased from RuiKemei (Chengdu, China). Sperm density was adjusted to $1 \times 10^6 - 2 \times 10^6$ sperm per ml with buffer solution (volume together about 50 μl). Acidizing solution (100 μl) was added into sperm buffer solution and vibrated mixture. Acidizing pause time did not exceed 30 s. Acidifying sperm were taken no more than 30 s and 300 μl acridine orange dye was added. A DxFLEX flow cytometer (Beckman Coulter, Bria, CA, USA) was used to detect the sperm fluorescence signal. Each sample received more than 5000 sperm fluorescence signals. The percentage of red fluorescence in the sum of fluorescence was calculated by the built-in software, which was the DFI value (**Supplementary Figure 1**).

Sperm acrosome reaction test

Sperm density was adjusted to 1×10^6 sperm per ml with G-IVF PLUS and 1 ml sperm was placed in two control tubes and two H_2O_2 tubes. H_2O_2 tubes were added 2 μl of 20 mmol l^{-1} H_2O_2. Sperm was incubated at 37°C, 5% CO_2, and 95% air humidity for 3 h. A kit for the determination of induced acrosome reaction was purchased from Bred (Shenzhen, China). One control tube and one H_2O_2 tube were protected from light and 2.5 μl of calcium ion carrier was added. Dimethyl sulfoxide (DMSO; 2.5 μl) was added to the remaining control tube and H_2O_2 tube. After treatment, an appropriate amount of spermatozoa was taken on the slide and dried at room temperature. Fluorescent conjugate (50 μl) for the acrosome reaction was added to the smear and incubated for 60 min. The smear was then observed under a fluorescent microscope (Zeiss, Oberkochen, Germany). The number of spermatozoa with an acrosome reaction in each smear well was recorded and divided by the total number of spermatozoa counted in that well, and this value was known as the acrosome incidence rate of the tube. At least 400 spermatozoa were counted in each smear window. The calculation is as follows:

Control tube's induced acrosome response rate (%) = control tube's calcium addition-induced tube acrosome response rate – control tube's uninduced tube acrosome response rate.

H_2O_2 tube's induced acrosome reaction rate (%) = H_2O_2 treatment tube's calcium addition-induced tube acrosome reaction rate – H_2O_2 treatment tube's uninduced tube acrosome reaction rate.

Protein extraction and Western blot

The appropriate amount of radioimmunoprecipitation assay (RIPA) lysate was added to sperm according to the amount of sperm retained, and then the appropriate amount of phenylmethanesulfonyl fluoride (PMSF) and phosphatase inhibitor was added. After mixing well with a vortex shaker, samples were lysed on ice for 30 min, shaking every 5 min. The lysates were then centrifuged at 7776*g* to remove any sperm debris and the supernatant protein was kept at −20°C. Protein concentration was determined by a BCA kit (Beyotime, Shanghai, China). Protein (30 μg) was added to 5× loading buffer and denatured by heating in a metal bath at 99°C for 10 min. Protein was separated by sodium dodecyl sulfate-polyacrylamide gel electrophoresis (SDS-PAGE) and pre-stained with protein markers to indicate protein molecular weight. The proteins were transferred to a polyvinylidene fluoride (PVDF) membrane (Millipore, Billerica, MA, USA) and blocked with 5% skim milk for 1.5 h, followed by primary antibody incubation overnight at 4°C. The membrane was then washed by Tris-buffered saline with 0.1% Tween-20 (TBST) for three times of 10 min each, and incubated with the corresponding secondary antibody for 1 h at room temperature, followed by three more washes. The protein blots were treated using an enhanced chemiluminescence kit (ECL) and were then qualitatively assessed using a gel imaging system (Bio-Rad, Hercules, CA, USA). ImageJ software (National Institutes of Health, New York, NY, USA) was used to analyze the images.

Primary antibodies were diluted in TBST as follows: glyceraldehyde-3-phosphate dehydrogenase (GAPDH; 1:10 000), PKARII (1:5000), AKAP4 (1:1000), heat shock protein A2 (HSPA2; 1:5000), proliferating cell nuclear antigen (PCNA; 1:1000), phospho-extracellular regulated protein kinases (p-ERK) 1/2 (1:1000), Phosphatidylinositol 3-kinase (PI3K; 1:1000), SPA17 (1:1000), p-AKT (1:1000), and AKT (1:1000). Secondary antibodies were diluted 1:10 000 in TBST.

Sperm RNA extraction and reverse transcription-polymerase chain reaction (RT-PCR)

Total RNA was extracted by lysing the sperm using MonAmp™ RNA Extraction Reagent (Monad, Wuhan, China). The RNA concentration was determined by NanoDrop2000 ultra-micro spectrophotometer (Thermo Fisher Scientific, Waltham, MA, USA). Reverse transcription was performed according to the required amount of 1 μg RNA to obtain cDNA with MonAmp™ Reverse Transcription Kit. A 10 μl reaction system was prepared using MonAmp™ ChemoHS qPCR Mix as follows: 5 μl MonAmp™ ChemoHS qPCR Mix, 1 μl cDNA of the specimen to be tested, 0.5 μl primer, and 3.5 μl triple distilled water. PCR instrument settings were predenaturation at 95°C for 10 min, denaturation at 95°C for 10 s, and annealing and extension at 60°C for 30 s. It repeated for 40 times. After $2^{-\Delta\Delta CT}$ analysis, the data were normalized to the internal reference *GAPDH* values. The primer sequences for the reactions were shown previously.

Statistical analyses

Statistical analyses were performed using the Statistical Package for the Social Sciences software, version 25 (SPSS Inc., Chicago, IL, USA). First, nonparametric tests (one-sample Kolmogorov–Smirnov test) were used to determine whether analyzed parameters were normally distributed. For the normal distribution, measurement data were presented as mean ± standard deviation (s.d.) and counting data were presented as count (percentage, %). For nonnormal distribution, data were presented as median (interquartile range [IQR]). Differences between normally distributed groups were compared through Student's *t*-test, Mann–Whitney U test, Chi-square test, or one-way analysis of variance (ANOVA) test. Nonnormal distributed groups were compared through normalized Wilcoxon rank sum test statistic. All tests of the hypothesis were two-sided, and $P < 0.05$ was considered to indicate

statistical significance. All experiments were repeated at least three times with more than three independent samples per group.

RESULTS

Comparison of IVF and pregnancy outcomes between H-DFI and L-DFI patients

Following inclusion criteria filtering, a total of 179 male patients were enrolled in this study and divided into L-DFI (n = 137) and H-DFI (n = 42) groups. A statistical analysis of the two couples was carried out at baseline. Female data collected included age, body mass index (BMI), follicle-stimulating hormone (FSH), luteinizing hormone (LH), estradiol (E_2), endometrial thickness on human chorionic gonadotropin (hCG) day, and the number of oocytes retrieved during their cycle. Male data collected included results from routine semen analysis and sperm morphology testing of male patients on the day of oocyte retrieval. There was no statistical difference between the two groups in all the above basic female indexes (**Supplementary Table 1**). There were statistical differences in the progressive motility (PR) sperm (mean ± s.d.: 44.2% ± 17.6% *vs* 36.7% ± 14.8%, P = 0.016) and normal sperm morphology rate (mean ± s.d.: 7.2% ± 1.3% *vs* 5.2% ± 2.1%, P < 0.001) between the L-DFI group and H-DFI group of male patients. Compared with the L-DFI group, the H-DFI group had a lower PR sperm rate and higher sperm morphology abnormalities (**Table 1**). There was no statistically significant difference in sperm concentration, immobile (IM) sperm, and the total sperm motility rate (progressive + nonprogressive motility [PR + NP]), but all the data in the H-DFI group trended worse than those in the L-DFI group, which showed that the overall semen quality decreased.

Embryo culture from the two groups was recorded and the outcomes of transplanted pregnancies were followed up. In the fresh cycle, 83 male patients in the L-DFI group were transplanted at the cleavage stage. In the H-DFI group, 26 cases were transplanted at the cleavage stage. Follow-up pregnancy outcomes showed that in the L-DFI group, there were 41 cases of clinical pregnancy, 4 cases of miscarriage, and 37 cases of live birth. However, in the H-DFI group, there were 13 cases of clinical pregnancy, 3 cases of miscarriage, and 10 cases of live birth. There was a statistical difference in the fertilization rate (81.0% *vs* 75.9%, P = 0.011) between the L-DFI group and H-DFI group (**Table 2**), but the remaining items were not statistically different in the two groups. Therefore, the results of the trials proved that female patients in the H-DFI group had worse pregnancy outcomes than those in the L-DFI group. Compared with the L-DFI group, the H-DFI group had a higher miscarriage rate (21.4% *vs* 9.8%, P = 0.354).

Elevated expression of SPA17 at the mRNA and protein level in the H-DFI group

To explore the specific effects of sperm DNA fragmentation formation on sperm-related functions, we further analyzed the sperm proteins that were susceptible to oxidative stress damage during sperm DNA fragmentation. We selected HSPA2, heat shock protein 90 (HSP90), angiotensin-converting enzyme (ACE), PCNA and SPA17 for detection by RT-PCR and Western blot. RT-PCR results showed that the mRNA levels (mean±s.d.) of *HSPA2* (9.9 ± 8.9 *vs* 61.2 ± 57.9, P = 0.026), *PCNA* (1.5 ± 0.9 *vs* 3.1 ± 1.6, P = 0.027), *ACE* (1.1 ± 1.0 *vs* 4.9 ± 3.8, P = 0.035), and *SPA17* (3.7 ± 3.1 *vs* 12.6 ± 9.7, P = 0.033) in the L-DFI group and H-DFI group, respectively, were significantly different. The mRNA levels of *HSPA2*, *PCNA*, *ACE*, and *SPA17* were abnormal in the H-DFI group, while *HSP90* expression showed no difference between the two groups (P > 0.05). To further detect the protein expression of the relevant genes, we selected 4 semen samples each from the H-DFI and L-DFI groups, and then detected the expression of corresponding proteins by Western blot (**Figure 1a**). Western blot results showed that SPA17 protein expression was increased in H-DFI sperm compared with that in L-DFI sperm (**Figure 1b**; P < 0.05). We repeated the Western blot of SPA17 with 8 semen samples each, and the results were consistent with those before (**Figure 1c** and **1d**).The expression of HSPA2 and PCNA did not significantly change between the two groups (both P > 0.05).

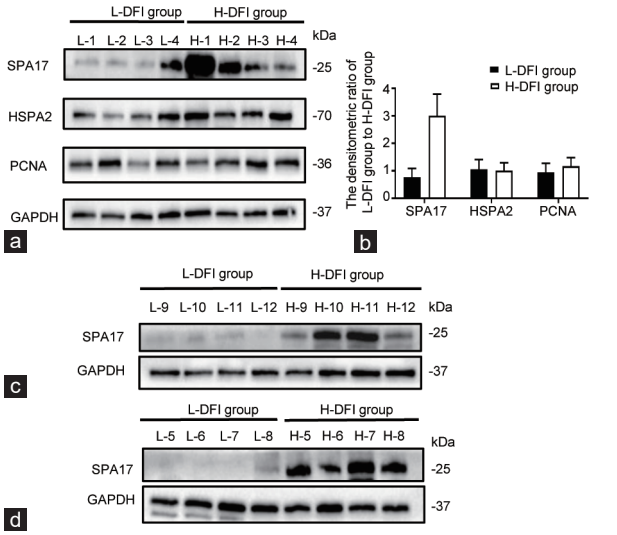

Figure 1: Relative expression of HSPA2, PCNA, SPA17 protein in the L-DFI and H-DFI groups. (**a**) Western blot analysis and (**b**) densitometric ratio histogram of HSPA2, PCNA and SPA17 with 4 semen samples of L-DFI (L-1 to L-4) and H-DFI (H-1 to H-4) groups each. Western blot analysis of SPA17 with 4 semen samples of L-DFI and H-DFI groups each, (**c**) L-9 to L-12, and H-9 to H-12, and (**d**) L-5 to L-8, and H-5 to H-8 in the L-DFI and H-DFI groups. We selected 12 semen samples in the L-DFI (L-1 to L-12) and H-DFI (H-1 to H-12) groups each. $^{**}P$ < 0.01. Data is presented as mean ± standard deviation. HSPA2: heat shock protein A2; PCNA: proliferating cell nuclear antigen; SPA17: sperm protein antigen 17; H-DFI: high sperm DNA fragmentation index; L-DFI: low sperm DNA fragmentation index; GAPDH: glyceraldehyde-3-phosphate dehydrogenase.

Table 1: Semen parameters between low sperm DNA fragmentation index and high sperm DNA fragmentation index groups

Characteristic	*L-DFI group (n=137)*	*H-DFI group (n=42)*	*t/Z*	*P*
Age (year), median (IQR)	31 (33–28)	31 (35–29)	–1.756	0.079
Sperm concentration (×10^6 ml^{-1}), median (IQR)	45.1 (66.9–30.9)	54.6 (81.7–31.9)	–0.879	0.379
PR sperm (%), mean±s.d.	44.2±17.6	36.7±14.8	–2.445	0.016
IM sperm (%), mean±s.d.	43.8±20.1	49.4±19.8	1.545	0.124
PR + NP sperm (%), mean±s.d.	56.2±20.1	50.6±19.8	–1.545	0.124
Normal sperm morphology (%), mean±s.d.	7.2±1.3	5.2±2.1	–7.338	<0.01

PR: progressive motility; IM: immobile; PR + NP: progressive + nonprogressive motility; H-DFI: high sperm DNA fragmentation index; L-DFI: low sperm DNA fragmentation index; *t/Z*: statistical value of Student's *t*-test or values of the normalized Wilcoxon rank sum test statistic; IQR: interquartile range

Table 2: Embryo cultures and *in vitro* fertilization outcomes between low sperm DNA fragmentation index and high sperm DNA fragmentation index groups

Characteristic	*L-DFI (n=137)*	*H-DFI (n=42)*	χ^2	*P*
Fertility rate (%)	81.0	75.9	6.415	0.011
Cleavage rate (%)	100.0	100.0	-	-
2PN fertility rate (%)	63.9	61.1	1.345	0.246
2PN cleavage rate (%)	99.7	99.8	-	-
Good-quality embryos rate (%)	31.5	32.5	0.126	0.723
Clinical pregnancy rate (%)	49.4	51.9	0.049	0.825
Miscarriage rate (%)	9.8	21.4	-	0.354
Live birth rate (%)	42.4	34.3	0.732	0.392

Fertility rate (%): fertility total eggs/retrieved total eggs; 2PN fertility rate (%): 2PN fertility total eggs/retrieved total eggs; cleavage rate (%): cleavage embryo/fertility total eggs; 2PN cleavage rate (%): 2PN cleavage embryo/2PN fertility total eggs; good-quality embryo rate (%): good-quality embryo/2PN fertility total eggs; clinical pregnancy rate (%): pregnant women/transplant women; miscarriage rate (%): miscarriage couples/clinical pregnancies; live birth rate (%): live birth couples/transplant couples. H-DFI: high sperm DNA fragmentation index; L-DFI: low sperm DNA fragmentation index; 2PN: 2 pronucleus; -: no value

Reduced AKAP4 and PKARII protein expression in H-DFI sperm

Since the significant elevation in protein expression of SPA17 in the H-DFI group, embryo culture data and clinical pregnancy outcomes suggested that the changes in SPA17 expression led to differences in fertilization rates between the two groups. The study further examined the expression of related proteins in the cAMP-PKA pathway, including PKARII, AKAP4, and downstream proteins PI3K, extracellular signal-regulated kinase of phosphorylation (p-ERK), AKT, and p-AKT by Western blot (**Figure 2a**). Western blot results showed that SPA17 expression was elevated in H-DFI sperm (**Figure 2b**; $P < 0.05$). The protein expressions (mean ± s.d.) of both AKAP4 (1.0 ± 0.2 *vs* 0.3 ± 0.1, $P = 0.013$) and PKARII (1.0 ± 0.2 *vs* 0.3 ± 0.1, $P = 0.016$) were decreased in the H-DFI group (**Figure 2a**–**2d**; both $P < 0.05$). The protein expression of PI3K, p-ERK, p-AKT, and AKT did not show significant differences (**Figure 2e**–**2i**; all $P > 0.05$).

H_2O_2 increased the expression of sperm SPA17 protein and suppressed AKAP4 and PKARII protein expression

Sperm were treated with different concentrations of H_2O_2 to simulate the damage of sperm induced by oxidative stress during sperm DFI formation. To clarify the relationship between sperm proteins of SPA17, AKAP4, and PKARII, and the occurrence of sperm DNA fragmentation, fresh semen was collected from the L-DFI group and the sperm density was adjusted to 1×10^6 sperm per ml with G-IVF PLUS. The H_2O_2 concentrations in the treatment group were 20 μmol l^{-1}, 40 μmol l^{-1} and 80 μmol l^{-1}, respectively (**Figure 3a** and **3b**), and the control group was routinely treated according to the manufacturer's instructions. Each sample was also incubated for 3 h in an incubator at 37°C, 5% CO_2, and 95% air humidity. Compared with the control group, the protein had no significant change at the H_2O_2 concentration of 20 μmol l^{-1}. As the concentration increased to 40 μmol l^{-1} and 80 μmol l^{-1}, the amount of sperm SPA17 protein increased significantly, while the amount of AKAP4 and PKARII protein decreased significantly (**Figure 3c**–**3e**; all $P < 0.05$). The differences in all three proteins were statistically significant, and with the increase in H_2O_2 concentration, the change of protein content changes significantly in a concentration-dependent manner.

H_2O_2 treatment inhibits sperm capacitation

According to clinical data, the fertilization rate of female patients in the H-DFI group decreased significantly ($P = 0.011$; **Table 2**). Previous results also indicated that the expressions of PKA and AKAP4 decreased in the H-DFI group and H_2O_2 treatment group. Therefore, the study further investigated the acrosome reaction ability of sperm after H_2O_2 treatment. Sperm were treated with 40 μmol l^{-1} H_2O_2 as described previously, and the acrosome reaction was induced with the calcium ionophore A23187 according to the Sperm Acrosome Reaction Detection Kit. The results proved that H_2O_2 treatment of sperm hindered the sperm capacitation process and reduced sperm acrosomal reaction. The difference in the rate of acrosomal reactions between the two groups was found to be statistically significant. The occurrence of an acrosomal reaction in spermatozoa significantly increased after calcium ionophore A23187 induction and the rate (mean ± s.d.) of induced acrosomal reactions in control-treated tubes was 34.2% ± 6.9% (**Figure 4a** and **4b**). However, the number of acrosome reaction induced by calcium ions was less after H_2O_2 treatment, and the rate of induced acrosomal reactions (mean ± s.d.) in H_2O_2-treated tubes was 4.9% ± 4.4% (**Figure 4c** and **4d**). The difference between the two tubes was statistically significant (**Figure 4e**; $P < 0.05$). These results indicated that H_2O_2 treatment reduced the occurrence of acrosome reactions.

DISCUSSIONS

Oxidative stress is a known cause of sperm damage, which is closely related to the formation of sperm DFI.[7] There is also a high correlation between H-DFI sperm and abnormalities in sperm morphology and sperm motility.[37] Some studies have shown a high overlap between the H-DFI populations and patients with teratozoospermia and asthenozoospermia.[38,39] In this study, we found that the H-DFI group exhibits an increase in the rate of abnormal sperm morphology accompanied by a decrease in the total number of forward motile sperm compared to the sperm in the L-DFI group. These abnormal sperm are related to the elevated formation of ROS during sperm DNA fragmentation. When a large amount of ROS acts on sperm DNA, the bases adduct 8-hydroxy-2'-deoxyguanosine (8OHdG) is produced. The formation of 8OHdG is strongly correlated with the result of DNA fragmentation.[40] ROS also attacks sperm mitochondrial DNA. Mitochondrial dysfunction leads to a decrease in sperm adenosine triphosphate (ATP) affecting sperm motility.[41] Furthermore, there are binding sites for ROS products on protamine-like proteins in the DNA structure of sperm, and their binding can lead to reduced chromatin agglutination and poor chromatin concentration, which results in abnormal sperm head morphology.[42] Ultimately, this leads to a decrease in overall sperm quality. Salmani *et al.*[43] showed that decreased expression of sperm proteins HSPA2, HSP90, and PCNA in their H-DFI population was closely related to sperm quality, and this study has also examined the expression of these three proteins in both groups of male patients in a follow-up experiment.

It is clear from the study data that ROS not only causes the breakage of sperm DNA but also affects sperm quality. In recent years, the number of H-DFI male patients undergoing assisted reproduction treatment has increased, and there has been discussion as to whether H-DFI sperm affects pregnancy outcomes in IVF. According to the clinical outcomes observed in this study, female patients in the H-DFI group have worser outcomes compared to the L-DFI group when assessing the results of fresh IVF cycles, especially when looking at the fertilization rate. In similar studies targeting sperm DFI,[44–46] the rate of "excellent" embryos, as well as the pregnancy rate, was significantly reduced. This suggests that the sperm DFI is an important factor in the clinical outcomes of assisted reproduction. However, this factor is not significant in intracytoplasmic sperm injection (ICSI).[47] Chi *et al.*[48]

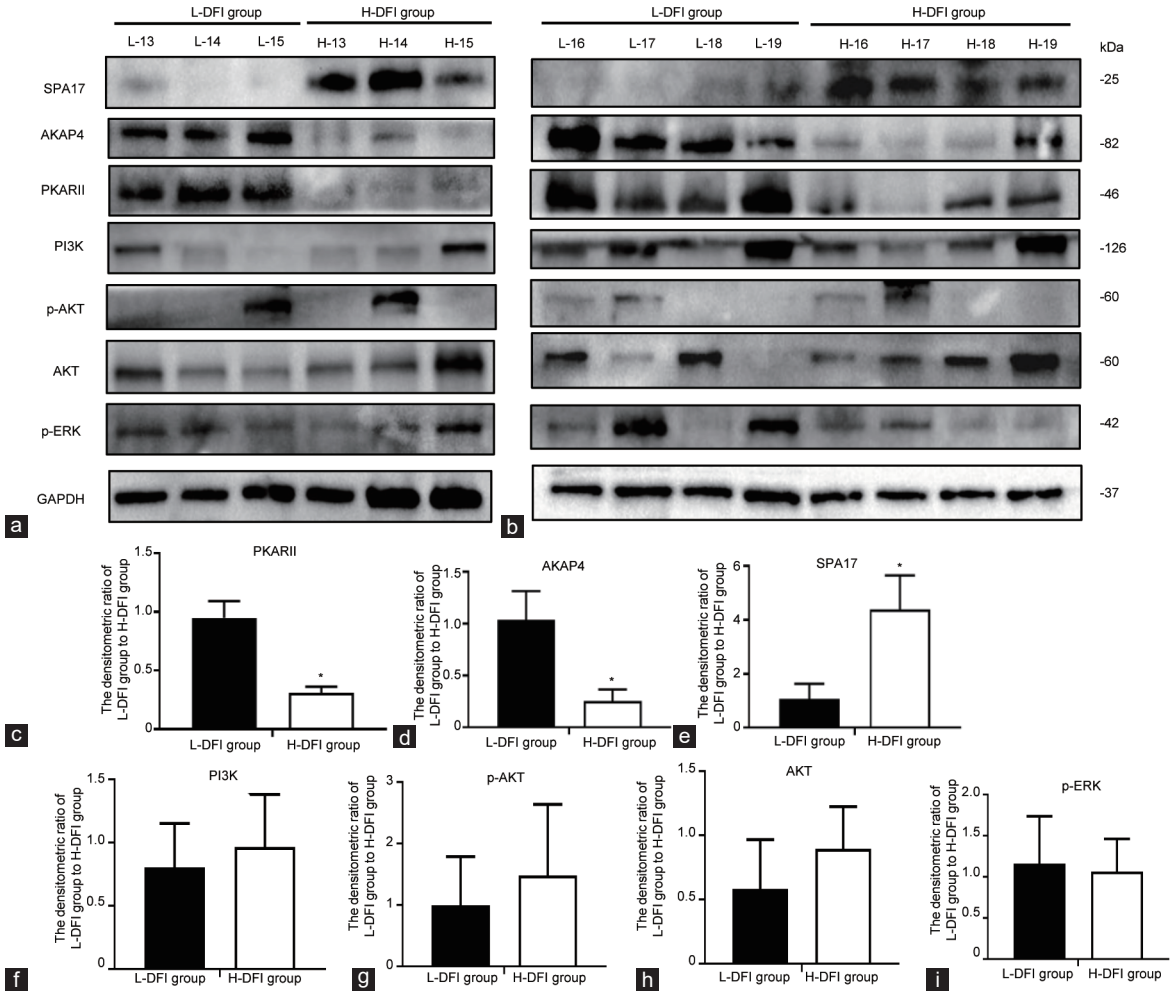

Figure 2: Relative expressions of PKA-associated protein in L-DFI and H-DFI groups. Western blot analysis of PKA-associated protein (**a**) with 3 semen samples of L-DFI (L-13 to L-15) and H-DFI (H-13 to H-15) groups, respectively, and (**b**) with 4 semen samples of L-DFI (L-15 to L-19) and H-DFI (H-15 to H-19) groups, respectively. Histograms demonstrated the densitometric ratio of (**c**) PKARII, (**d**) AKAP4, (**e**) SPA17, (**f**) PI3K, (**g**) p-AKT, (**h**) AKT, and (**i**) p-ERK in L-DFI and H-DFI groups. We selected 7 semen samples in the L-DFI (L-13 to L-19) and H-DFI (H-13 to H-19) groups, respectively. $^{*}P < 0.05$. Data are presented as mean ± standard deviation. PKA: protein kinase A; AKAP: a-kinase anchoring proteins; PI3K: phosphoInositide-3 kinase; AKT: protein kinase B; p-AKT: phosphorylated protein kinase B; p-ERK: extracellular signal-regulated kinase of phosphorylation; H-DFI: high sperm DNA fragmentation index; L-DFI: low sperm DNA fragmentation index; GAPDH: glyceraldehyde-3-phosphate dehydrogenase.

have shown that ICSI's selection of motile and morphologically normal sperm for injection into the oocytes greatly reduces the clinical consequences associated with sperm abnormalities. Therefore, this study further investigates the causes and molecular mechanisms, leading to decreased fertilization rates during IVF-ET.

The role of ROS is to participate in activating the cAMP-PKA pathway, increasing plasma membrane fluidity, and inducing cholesterol oxidation. ROS is produced at a relatively higher level in H-DFI sperm. When ROS is excessive, lipids oxidation on the plasma membrane produces a class of electrophilic aldehyde byproducts, such as 4-hydroxynonenal (4-HNE), acrolein (ACR), and malondialdehyde.[41] These aldehydes are highly likely to react with macromolecules (*e.g.*, proteins) to form stable products that lead to a range of abnormal physiological responses.[33] Not all sperm proteins have sites for interaction with electrophilic aldehydes, but a recent study identified related proteins in sperm. Hall *et al.*[49] found that HSP90 and arylsulfatase A (ARSA) could react with 4-HNE and ACR in horse sperm. HSP90 protein was considered in a previous study[50] to be related to sperm quality and thought to be involved in sperm motility. Bromfield *et al.*[51] identified 4-HNE binding sites on HSPA2. Experiments by Nixon's group showed decreases in the protein content of both AKAP4 and its precursor substance proAKAP4 in the presence of topical oxidants.[32] Baker *et al.*[33] found that 4-HNE had an activating effect on PKA, but high concentrations of 4-HNE caused a significant decrease in PKA activity, suggesting that PKA interacts with 4-HNE.

To investigate the changes in sperm function affected by ROS in H-DFI, especially in fertilization function, the study has examined the mRNA levels and protein expressions of HSPA2, PCNA, ACE, HSP90, and SPA17. The results showed that mRNA levels of *HSPA2*, *ACE*, *PCNA*, and *SPA17* were abnormal in the H-DFI population. Only SPA17 was increased at the protein level. There was no difference in HSPA2 and PCNA protein expression between the two groups. HSPA2 formed a complex with ARSA and sperm adhesion molecule 1 (SPAM1) during sperm–egg binding. It promoted the assembly, localization, and stabilization of the zona pellucida (ZP) receptor-zona pellucida complex on the surface of the sperm acrosome, which in turn ensures correct

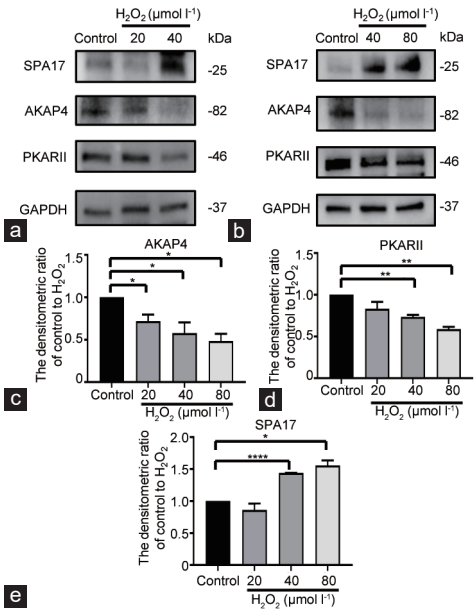

Figure 3: The protein expression of SPA17, AKAP4 and PKARII after H_2O_2 treatment of semen from the L-DFI group. Western blot analysis of SPA17, AKAP4 and PKARII (**a**) after 20 μmol l^{-1} and 40 μmol l^{-1} H_2O_2 treatment, and (**b**) after 40 μmol l^{-1} and 80 μmol l^{-1} H_2O_2 treatment. Histograms demonstrated the densitometric ratio of (**c**) AKAP4, (**d**) PKARII, and (**e**) SPA17. $^{*}P < 0.05$; $^{**}P < 0.01$; $^{***}P < 0.001$; $^{****}P < 0.0001$. Data are presented as mean ± standard deviation. SPA17: sperm protein antigen 17; PKA: protein kinase A; AKAP: A-kinase anchoring proteins; L-DFI: low sperm DNA fragmentation index; GAPDH: glyceraldehyde-3-phosphate dehydrogenase.

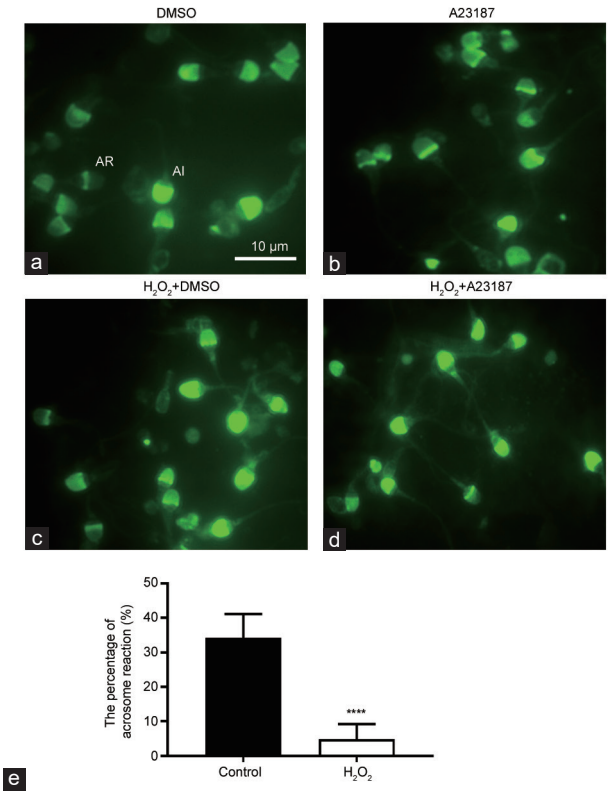

Figure 4: Evaluation of the human sperm acrosome reaction after 40 μmol l^{-1} H_2O_2 treatment and control. AR indicates capacitated and acrosome-reacted sperm, while AI indicates uncapacitated sperm. (**a**) Control tubes added DMSO. (**b**) Control tubes added calcium ionophore A23187. (**c**) H_2O_2 treatment group with DMSO. (**d**) H_2O_2 treatment group with calcium ionophore A23187. (**e**) Histograms demonstrated the acrosome reaction rate of sperm induces by calcium ionophore A23187. $^{****}P < 0.0001$. Data are presented as mean ± standard deviation. AR: acrosome reaction; AI: acrosome integrity; DMSO: dimethyl sulfoxide.

sperm–egg recognition.[52] When HSPA2 expression was reduced, it led to impaired sperm–egg recognition and decreased fertilization rate. At high ROS levels, the function of the HSPA2-SPAM1-ASRA complex was reduced by oxidation of the aldehydes produced by oxidation, but the protein content of the complex does not change significantly altered. Although a binding site of 4-HNE was found on HSPA2, 4-HNE did not affect the HSPA2 protein expression.[51] This study is consistent with our Western blot results. At the mRNA level, the results showed abnormal mRNA levels of *HSPA2* and *PCNA* was abnormal in the H-DFI group, which was differed from the results of Salmani *et al.*[43] Salmani concluded that the protein content of sperm HSP90, HSPA2, and PCNA decreased as sperm DFI increased and sperm quality decreased. This is due to the fact that the semen quality of male patients remained within the normal range and did not meet the diagnostic criteria for teratozoospermia and asthenozoospermia. Therefore, there is no difference in protein expression.

The expression of SPA17 protein was increased in the H-DFI group. The study further investigated this finding by observing changes in the expression of AKAP4, a protein that binds to SPA17 and PKA protein and is involved in sperm capacitation. The current study suggests that SPA17 may regulate sperm maturation, capacitation, acrosome response, and interaction with oocyte zona pellucida during fertilization.[31] The study has found that when sperm function is decreased, then SPA17 is increased. SPA17 forms a complex with AKAP-binding proteins, but the role it plays in sperm function is unclear.[31] The role of sperm proteins AKAP4 and PKA is well understood. AKAP4 mainly serves as a scaffolding protein for integrated signaling reactions, helping each reaction proceed independently and synergistically.[53] The important protein bound to AKAP4 during sperm capacitation is PKA. AKAP can serve as a platform for PKA to interact with substrates. PKA activation by cAMP can trigger the phosphorylation of downstream proteins, such as PI3K and phosphatidylinositol biphosphate (PIP2), to promote sperm capacitation and complete sperm HAM.[17] Therefore, AKAP4 and PKA are crucial for sperm motility and fertilization. However, AKAP4 has been shown to be very sensitive to 4-HNE. Nixon *et al.*[32] experiment found that the protein content of AKAP4, and its precursor substance proAKAP4, decreased under the influence of external oxidants. PKA protein can also interact with 4-HNE. In the Baker *et al.*[33] 4-HNE had a dual effect on PKA. Sperm PKA activity decreased significantly at high concentration of 4-HNE. Low concentrations of 4-HNE can activate PKA and subsequently increase sperm phosphorylation levels, a mechanism utilized by spermatozoa to produce endogenous ROS.

Given the role and function of AKAP4 and PKA in sperm, the study has compared PKARII, AKAP4, and its downstream proteins PI3K, ERK, and AKT in the sperm of two groups of male patients. The results showed that AKAP4 and PKARII decreased significantly in the H-DFI population, and the rest of the proteins were not significantly different between the two groups. AKAP4 was lost by a large amount of ROS. Due to the reduction of the carrier protein AKAP, free SPA17 was increased in H-DFI population and the amount of SPA17 protein was increased. This is similar to the mouse study by Huang *et al.*,[54] showing increased SPA17 expression in *AKAP4*-knockout mice and decreased SPA17 protein in wild-type mice. This suggests that

there is an interaction between AKAP4 and SPA17. Regarding the decrease in PKA protein, although Baker *et al.*[33] concluded that the amount of protein did not change, another study of oxidative stress in cardiomyocytes[55] found that both PKA and AKAP showed protein loss in cardiomyocytes under the influence of H_2O_2 and that there was a significantly correlation with the duration and concentration of H_2O_2. The variation of PKA protein content in sperm is also related to the duration and concentration of H_2O_2. H-DFI sperm were exposed to high ROS levels for a long time, and AKAP4 and PKA were affected by oxidized substances, causing protein loss and impaired function, increased SPA17 protein, reduced sperm phosphorylation levels, and blocked sperm capacitation, which ultimately led to the reduced fertilization rate observed in H-DFI population. AKAP4 was also mainly expressed in the caudal fibrous sheath of spermatozoa, recruiting PKA to promote local phosphorylation and participating in the activation of the sperm flagellum.[56] A previously published study reported that a decreased level of AKAP4 expression affected sperm motility.[23] Therefore, this study concluded that it was the reason for the decreased forward motility of spermatozoa in H-DFI population.

To further validate the preliminary experimental results, the study employed a method in which oxidant interventions were added to normal sperm DFI samples. Different concentrations of H_2O_2 were added separately to simulate the high-ROS environment observed in H-DFI sperm.[57] Protein expression in the H_2O_2-treated sperm was examined. Treatment with different concentrations of H_2O_2 revealed a gradual decrease in the expression of AKAP4 and PKARII and a gradual increase in the expression of SPA17. These results were consistent with previous findings of this team. In addition, the study examined the induced acrosome reaction in H_2O_2-treated sperm and untreated sperm, and found that the ability of sperm to induce an acrosome reaction was decreased significantly under H_2O_2 treatment. Therefore, elevating oxidants affected AKAP4 and PKA proteins in spermatozoa and blocked sperm capacitation. The decrease in PKA resulted in inadequate tyrosine phosphorylation of sperm, causing decrease in sperm acrosome response and fertilization capacity. This was demonstrated by an increase in SPA17, which predicted the fertilization ability of sperm after oxidation. Meanwhile, the increase in SPA17 expression was accompanied by a decrease in sperm capacitation, which also represented a decrease in fertilizing ability.

ROS damage to sperm affects sperm functions and the genetic material of sperm. Altered sperm fertilization ability directly leads to a decrease in fertilization rate.[58] Sperm DFI has often been regarded as a clinical indicator of the level of oxidative stress in sperm. The relationship between sperm DFI and IVF outcomes has remained different by various parties. Due to the varying antioxidant capacities of different individuals, sperm DFI only reflects damage to sperm genetic material under oxidative stress and does not truly reflect the changes in various sperm functions. In this study, there was no statistical significance in the good-quality embryo rate, clinical pregnancy rate, and live birth rate between the two groups, which was related to the selection of women ≤38 years old in this study. The oocytes of young women have an outstanding ability to repair sperm DNA fragments. However, elderly female patients are less able to repair sperm DNA fragments. However, elderly female patients are less able to repair sperm DNA fragments, which may also be one of the reasons why many scholars believe that H-DFI sperm may affect the pregnancy outcomes of IVF.[59–61] In the future, the study will further increase the research on H-DFI sperm in elderly female patients by increasing the sample size. The study indicates that the increased SPA17 expression observed in H-DFI sperm is the sperm fertilization capacity indicator. Moreover, the decrease in sperm fertilization is due to the decreasing AKAP4 protein, leading to impairment of the cAMP-PKA pathway.

CONCLUSION

The results of this study suggest that elevated sperm DFI causes a decrease in sperm quality. The H-DFI group has a slightly worse clinical outcome than the L-DFI group, with a significantly lower fertilization rate. There is a trend towards an increased miscarriage rate in the H-DFI group. The study indicates that a possible explanation for the decreased fertilization rate observed in the H-DFI group is the loss of sperm AKAP4 and PKARII proteins, which results in impairment of the cAMP-PKA pathway in the sperm capacitation process, thus blocking sperm capacitation, and reducing the occurrence of acrosomal reactions. The loss of AKAP4 protein was accompanied by a significant increase in the expression of SPA17 protein in the H-DFI population.

AUTHOR CONTRIBUTIONS

KZ, XHX, and JFC designed the study. JW, NW, KZ, XHX, and JFC performed the experiments. KZ, XHX, JW, GL, and GMH analyzed the data. KZ drafted the paper. GL and XHX revised the paper. All authors read and approved the final manuscript.

COMPETING INTERESTS

All authors declare no competing interests.

ACKNOWLEDGMENTS

The authors thank all the patients who participated in this study. This study was supported by Hebei Natural Science Foundation (H2022206019), Science and Technology (S and T) Program of Hebei (21377721D), Hebei Province Medical Technology Tracking Project (GZ2021028), and Medical Science Research Project of Hebei Province (20170084, and 20211494).

Supplementary Information is linked to the online version of the paper on the *Asian Journal of Andrology* website.

REFERENCES

1 Tang L, Rao M, Yang W, Yao Y, Luo Q, *et al*. Predictive value of the sperm DNA fragmentation index for low or failed IVF fertilization in men with mild-to-moderate asthenozoospermia. *J Gynecol Obstet Hum Reprod* 2021; 50: 101868.
2 Borges E Jr., Zanetti BF, Setti AS, Braga D, Provenza RR, *et al*. Sperm DNA fragmentation is correlated with poor embryo development, lower implantation rate, and higher miscarriage rate in reproductive cycles of non-male factor infertility. *Fertil Steril* 2019; 112: 483–90.
3 Zhu XB, Chen Q, Fan WM, Niu ZH, Xu BF, *et al*. Sperm DNA fragmentation in Chinese couples with unexplained recurrent pregnancy loss. *Asian J Androl* 2020; 22: 296–301.
4 Yang H, Li G, Jin H, Guo Y, Sun Y. The effect of sperm DNA fragmentation index on assisted reproductive technology outcomes and its relationship with semen parameters and lifestyle. *Transl Androl Urol* 2019; 8: 356–65.
5 Lu JC, Jing J, Chen L, Ge YF, Feng RX, *et al*. Analysis of human sperm DNA fragmentation index (DFI) related factors: a report of 1010 subfertile men in China. *Reprod Biol Endocrinol* 2018; 16: 23.
6 Ferrigno A, Ruvolo G, Capra G, Serra N, Bosco L. Correlation between the DNA fragmentation index (DFI) and sperm morphology of infertile patients. *J Assist Reprod Genet* 2021; 38: 979–86.
7 Bisht S, Faiq M, Tolahunase M, Dada R. Oxidative stress and male infertility. *Nat Rev Urol* 2017; 14: 470–85.
8 Mostek A, Janta A, Majewska A, Ciereszko A. Bull sperm capacitation is accompanied by redox modifications of proteins. *Int J Mol Sci* 2021; 22: 7903.
9 O'Flaherty C. Redox regulation of mammalian sperm capacitation. *Asian J Androl* 2015; 17: 583–90.
10 Aitken RJ. Reactive oxygen species as mediators of sperm capacitation and pathological damage. *Mol Reprod Dev* 2017; 84: 1039–52.
11 Gazo I, Shaliutina-Kolesova A, Dietrich MA, Linhartova P, Shaliutina O, *et al*. The effect of reactive oxygen species on motility parameters, DNA integrity, tyrosine phosphorylation and phosphatase activity of common carp (*Cyprinus carpio* L.) spermatozoa. *Mol Reprod Dev* 2015; 82: 48–57.
12 Moreno-Irusta A, Dominguez E, Marín-Briggiler C, Matamoros-Volante A, Lucchesi O, *et al*. Reactive oxygen species are involved in the signaling of equine

sperm chemotaxis. *Reproduction* 2020; 159: 423–36.
13 Signorelli J, Diaz E, Morales PJ. Kinases, phosphatases and proteases during sperm capacitation. *Cell Tissue Res* 2012; 349: 765–82.
14 Finkelstein M, Etkovitz N, Breitbart HJ. Ca^{2+} signaling in mammalian spermatozoa. *Mol Cell Endocrinol* 2020; 516: 110953.
15 Baro Graf C, Ritagliati C, Stival C, Luque GM, Gentile I, *et al.* Everything you ever wanted to know about PKA regulation and its involvement in mammalian sperm capacitation. *Mol Cell Endocrinol* 2020; 518: 110992.
16 Burton K, McKnight GJ. PKA, germ cells, and fertility. *Physiology (Bethesda)* 2007; 22: 40–6.
17 Tsirulnikov E, Huta Y, Breitbart H. PKA and PI3K activities during capacitation protect sperm from undergoing spontaneous acrosome reaction. *Theriogenology* 2019; 128: 54–61.
18 Newell AE, Fiedler SE, Ruan JM, Pan J, Wang PJ, *et al.* Protein kinase A RII-like (R2D2) proteins exhibit differential localization and AKAP interaction. *Cell Motil Cytoskeleton* 2008; 65: 539–52.
19 Stival C, Ritagliati C, Xu X, Gervasi MG, Luque GM, *et al.* Disruption of protein kinase a localization induces acrosomal exocytosis in capacitated mouse sperm. *J Biol Chem* 2018; 293: 9435–47.
20 Torres-Quesada O, Mayrhofer JE, Stefan E. The many faces of compartmentalized PKA signalosomes. *Cell Signal* 2017; 37: 1–11.
21 Vizel R, Hillman P, Ickowicz D, Breitbart H. AKAP3 degradation in sperm capacitation is regulated by its tyrosine phosphorylation. *Biochim Biophys Acta* 2015; 1850: 1912–20.
22 Harrison DA, Carr DW, Meizel S. Involvement of protein kinase A and A kinase anchoring protein in the progesterone-initiated human sperm acrosome reaction. *Biol Reprod* 2000; 62: 811–20.
23 Moretti E, Scapigliati G, Pascarelli NA, Baccetti B, Collodel G. Localization of AKAP4 and tubulin proteins in sperm with reduced motility. *Asian J Androl* 2007; 9: 641–9.
24 Fang X, Huang LL, Xu J, Ma CQ, Chen ZH, *et al.* Proteomics and single-cell RNA analysis of *Akap4*-knockout mice model confirm indispensable role of *Akap4* in spermatogenesis. *Dev Biol* 2019; 454: 118–27.
25 Lea IA, Widgren EE, O'Rand MG. Association of sperm protein 17 with A-kinase anchoring protein 3 in flagella. *Reprod Biol Endocrinol* 2004; 2: 57.
26 Chiriva-Internati M, Gagliano N, Donetti E, Costa F, Grizzi F, *et al.* Sperm protein 17 is expressed in the sperm fibrous sheath. *J Transl Med* 2009; 7: 61.
27 Song Y, Qi X, Kang J, Wang X, Ou N, *et al.* Identification of new biomarkers in immune microenvironment of testicular germ cell tumour. *Andrologia* 2021; 53: e13986.
28 Zhou YT, Qiu JJ, Wang Y, Liu PC, Lv Q, *et al.* Sperm protein antigen 17 expression correlates with lymph node metastasis and worse overall survival in patients with breast cancer. *Front Oncol* 2019; 9: 710.
29 Arnaboldi F, Menon A, Menegola E, Di Renzo F, Mirandola L, *et al.* Sperm protein 17 is an oncofetal antigen: a lesson from a murine model. *Int Rev Immunol* 2014; 33: 367–74.
30 Richardson RT, Yamasaki N, O'Rand MG. Sequence of a rabbit sperm zona pellucida binding protein and localization during the acrosome reaction. *Dev Biol* 1994; 165: 688–701.
31 Frayne J, Hall LJ. A re-evaluation of sperm protein 17 (Sp17) indicates a regulatory role in an A-kinase anchoring protein complex, rather than a unique role in sperm-zona pellucida binding. *Reproduction* 2002; 124: 767–74.
32 Nixon B, Bernstein IR, Cafe SL, Delehedde M, Sergeant N, *et al.* A kinase anchor protein 4 is vulnerable to oxidative adduction in male germ cells. *Front Cell Dev Biol* 2019; 7: 319.
33 Baker MA, Weinberg A, Hetherington L, Villaverde AI, Velkov T, *et al.* Defining the mechanisms by which the reactive oxygen species by-product, 4-hydroxynonenal, affects human sperm cell function. *Biol Reprod* 2015; 92: 108.
34 O'Flaherty C, Matsushita-Fournier D. Reactive oxygen species and protein modifications in spermatozoa. *Biol Reprod* 2017; 97: 577–85.
35 Gardner DK, Schoolcraft WB. *In vitro* culture of human blastocyst. In: Jansen R, Mortimer D. Toward reproductive certainty: fertility and genetics beyond 1999. Carnforth: Parthenon Press; 1999. p378–88.
36 World Health Organization. WHO Laboratory Manual for the Examination and Processing of Human Semen. 5th ed. Geneva: WHO Press; 2010. p116–8.
37 Asadi A, Ghahremani R, Abdolmaleki A, Rajaei F. Role of sperm apoptosis and oxidative stress in male infertility: a narrative review. *Int J Reprod Biomed* 2021; 19: 493–504.
38 Palermo GD, Neri QV, Cozzubbo T, Rosenwaks Z. Perspectives on the assessment of human sperm chromatin integrity. *Fertil Steril* 2014; 102: 1508–17.
39 Aitken RJ, De Iuliis GN, Finnie JM, Hedges A, McLachlan RI. Analysis of the relationships between oxidative stress, DNA damage and sperm vitality in a patient population: development of diagnostic criteria. *Hum Reprod* 2010; 25: 2415–26.
40 De Iuliis GN, Thomson LK, Mitchell LA, Finnie JM, Koppers AJ, *et al.* DNA damage in human spermatozoa is highly correlated with the efficiency of chromatin remodeling and the formation of 8-hydroxy-2'-deoxyguanosine, a marker of oxidative stress. *Biol Reprod* 2009; 81: 517–24.
41 Aitken RJ, Whiting S, De Iuliis GN, McClymont S, Mitchell LA, *et al.* Electrophilic aldehydes generated by sperm metabolism activate mitochondrial reactive oxygen species generation and apoptosis by targeting succinate dehydrogenase. *J Biol Chem* 2012; 287: 33048–60.
42 Chen SJ, Allam JP, Duan YG, Haidl G. Influence of reactive oxygen species on human sperm functions and fertilizing capacity including therapeutical approaches. *Arch Gynecol Obstet* 2013; 288: 191–9.
43 Salmani S, Razi M, Sarrafzadeh-Rezaei F, Mahmoudian A. Testosterone amplifies HSP70-2a, HSP90 and PCNA expression in experimental varicocele condition: implication for DNA fragmentation. *Reprod Biol* 2020; 20: 384–95.
44 Gualtieri R, Kalthur G, Barbato V, Longobardi S, Di Rella F, *et al.* Sperm oxidative stress during *in vitro* manipulation and its effects on sperm function and embryo development. *Antioxidants (Basel)* 2021; 10: 1025.
45 Parrella A, Keating D, Cheung S, Xie P, Stewart JD, *et al.* A treatment approach for couples with disrupted sperm DNA integrity and recurrent ART failure. *J Assist Reprod Genet* 2019; 36: 2057–66.
46 Tello-Mora P, Hernandez-Cadena L, Pedraza J, Lopez-Bayghen E, Quintanilla-Vega B. Acrosome reaction and chromatin integrity as additional parameters of semen analysis to predict fertilization and blastocyst rates. *Reprod Biol Endocrinol* 2018; 16: 102.
47 Anifandis G, Bounartzi T, Messini CI, Dafopoulos K, Markandona R, *et al.* Sperm DNA fragmentation measured by Halosperm does not impact on embryo quality and ongoing pregnancy rates in IVF/ICSI treatments. *Andrologia* 2015; 47: 295–302.
48 Chi HJ, Kim SG, Kim YY, Park JY, Yoo CS, *et al.* ICSI significantly improved the pregnancy rate of patients with a high sperm DNA fragmentation index. *Clin Exp Reprod Med* 2017; 44: 132–40.
49 Hall SE, Aitken RJ, Nixon B, Smith ND, Gibb Z. Electrophilic aldehyde products of lipid peroxidation selectively adduct to heat shock protein 90 and arylsulfatase A in stallion spermatozoa. *Biol Reprod* 2017; 96: 107–21.
50 Ferlin A, Speltra E, Patassini C, Pati A M, Garolla A, *et al.* Heat shock proteinand heat shock factor expression in sperm: relation to oligozoospermia and varicocele. *J Urol* 2010; 183: 1248–52.
51 Bromfield EG, Aitken RJ, Anderson AL, McLaughlin EA, Nixon B. The impact of oxidative stress on chaperone-mediated human sperm-egg interaction. *Hum Reprod* 2015; 30: 2597–613.
52 Nixon B, Bromfield EG, Cui J, De Iuliis GN. Heat shock protein A2 (HSPA2): regulatory roles in germ cell development and sperm function. *Adv Anat Embryol Cell Biol* 2017; 222: 67–93.
53 Luconi M, Cantini G, Baldi E, Forti G. Role of a-kinase anchoring proteins (AKAPs) in reproduction. *Front Biosci (Landmark Ed)* 2011; 16: 1315–30.
54 Huang Z, Somanath PR, Chakrabarti R, Eddy EM, Vijayaraghavan S. Changes in intracellular distribution and activity of protein phosphatase PP1gamma2 and its regulating proteins in spermatozoa lacking AKAP4. *Biol Reprod* 2005; 72: 384–92.
55 Haushalter K, Schilling J, Song Y, Sastri M, Perkins G, *et al.* Cardiac ischemia-reperfusion injury induces ROS-dependent loss of PKA regulatory subunit RIα. *Am J Physiol Heart Circ Physiol* 2019; 317: H1231–42.
56 Gu L, Liu X, Yang J, Bai J. A new hemizygous missense mutation, c.454TC (p.S152P), in *AKAP4* gene is associated with asthenozoospermia. *Mol Reprod Dev* 2021; 88: 587–97.
57 Bader R, Ibrahim JN, Moussa M, Mourad A, Azoury J, *et al. In vitro* effect of autologous platelet-rich plasma on H_2O_2-induced oxidative stress in human spermatozoa. *Andrology* 2020; 8: 191–200.
58 Liang X, Mao Y, Wang Y, Liu S, Yan J. Female age affects the utility of sperm DNA fragmentation in predicting IVF and ICSI outcomes. *Reprod Biomed Online* 2019; 39: 955–62.
59 Newman H, Catt S, Vining B, Vollenhoven B, Horta F. DNA repair and response to sperm DNA damage in oocytes and embryos, and the potential consequences in ART: a systematic review. *Mol Hum Reprod* 2022; 28: gaab071.
60 Setti AS, Braga D, Provenza RR, Iaconelli A Jr, Borges E Jr. Oocyte ability to repair sperm DNA fragmentation: the impact of maternal age on intracytoplasmic sperm injection outcomes. *Fertil Steril* 2021; 116: 123–9.
61 Marchetti F, Essers J, Kanaar R, Wyrobek AJ. Disruption of maternal DNA repair increases sperm-derived chromosomal aberrations. *Proc Natl Acad Sci U S A* 2007; 104: 17725–9.

Supplementary Table 1: Baseline characteristics of female between the low sperm DNA fragment index and high sperm DNA fragment index groups

Characteristic	*L-DFI (n=137)*	*H-DFI (n=42)*	*t/Z*	*P*
Age (year), median (IQR)	30 (32–28)	31 (34–29)	3.847	0.146
BMI (kg m^{-2}), mean±s.d.	23.81±3.84	24.58±3.13	1.064	0.289
FSH (mIU ml^{-1}), median (IQR)	6.93 (7.98–5.83)	6.62 (7.67–5.91)	0.601	0.740
LH (mIU ml^{-1}), median (IQR)	5.53 (6.34–4.56)	5.55 (6.65–4.39)	0.693	0.707
E_2 (pg ml^{-1}), median (IQR)	40.01 (50.10–29.52)	44.50 (55.29–31.46)	2.497	0.287
Endometrial thickness on HCG day (mm), median (IQR)	11 (10–13)	11 (9–13)	3.322	0.190
Retrieved oocytes, median (IQR)	11.5 (8.0–15.0)	13 (8.0–17.0)	0.623	0.732

L-DFI: low sperm DNA fragment index; H-DFI: high sperm DNA fragment index; BMI: body mass index; FSH: follicle-stimulating hormone; LH: luteinizing hormone; E_2: estradiol; HCG: human chorionic gonadotropin; s.d.: standard deviation; IQR: interquartile range

Supplementary Table 2: The DNA sequences of target gene

Target gene	*Forward primer*	*Reverse primer*
HSPA2	5'-GGCCCCGGCCTATTTCAACG-3'	5'-GGACACGTCGAAAGTGCCA-3'
HSP90	5'-GCTTGACCAATGACTGGGAAG-3'	5'-AGCTCCTACCAGTTATCCAGTA-3'
SPA17	5'-ATGTCGATTCCATTCTCCAACAC-3'	5'-ATTGTCCGGTTGCTCTCTCAG-3'
PCNA	5'-CCTGCTGGGATATTAGCTCCA-3'	5'-CAGCGGTAGGTGTCGAAGC-3'
ACE	5'-CCACGTCCCGGAAATATGAAG-3'	5'-AGTCCCCTGCATCTACATAGC-3'

HSPA2: heat shock protein A2; *PCNA*: proliferating cell nuclear antigen; *SPA17*: sperm protein antigen 17; *ACE*: angiotensin-converting enzyme; *HSP90*: angiotensin-converting enzyme

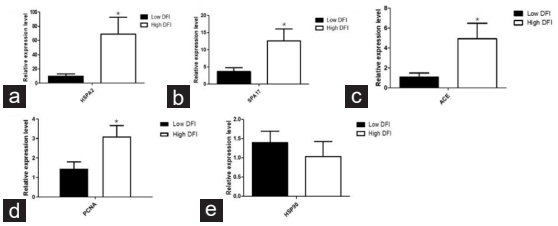

Supplementary Figure 1: RNA levels of (**a**) *HSPA2*, (**b**) *SPA17*, (**c**) *ACE*, (**d**) *PCNA*, and (**e**) *HSP90* in the L-DFI group and H-DFI group ($n = 9$ biological replicates, data presented as mean ± standard deviation; $^{*}P < 0.05$). *HSPA2*: heat shock protein A2; *PCNA*: proliferating cell nuclear antigen; *SPA17*: sperm protein antigen 17; ACE: angiotensin-converting enzyme; HSP90: angiotensin-converting enzyme.